

Structural Stability Of Detached Low Crested Breakwaters

Burcharth, Hans F.; Kramer, Morten; Lamberti, Alberto; Zanuttigh, Barbara

Published in:
Coastal Engineering

DOI (link to publication from Publisher):
[10.1016/j.coastaleng.2005.10.023](https://doi.org/10.1016/j.coastaleng.2005.10.023)

Publication date:
2006

Document Version
Publisher's PDF, also known as Version of record

[Link to publication from Aalborg University](#)

Citation for published version (APA):
Burcharth, H. F., Kramer, M., Lamberti, A., & Zanuttigh, B. (2006). Structural Stability Of Detached Low Crested Breakwaters. *Coastal Engineering*, 53(4), 381-394. <https://doi.org/10.1016/j.coastaleng.2005.10.023>

General rights

Copyright and moral rights for the publications made accessible in the public portal are retained by the authors and/or other copyright owners and it is a condition of accessing publications that users recognise and abide by the legal requirements associated with these rights.

- Users may download and print one copy of any publication from the public portal for the purpose of private study or research.
- You may not further distribute the material or use it for any profit-making activity or commercial gain
- You may freely distribute the URL identifying the publication in the public portal -

Take down policy

If you believe that this document breaches copyright please contact us at vbn@aub.aau.dk providing details, and we will remove access to the work immediately and investigate your claim.

Structural stability of detached low crested breakwaters

Hans F. Burcharth^{a,*}, Morten Kramer^a, Alberto Lamberti^b, Barbara Zanuttigh^b

^a Department of Civil Engineering, Aalborg University, Sohngaardsholmsvej 57, Aalborg, 9000, Denmark

^b DISTART Idraulica, Università di Bologna, viale del Risorgimento 2, 40136 Bologna, Italy

Accepted 24 October 2005

Available online 6 December 2005

Abstract

The aim of the paper is to describe hydraulic stability of rock-armoured low-crested structures on the basis of new experimental tests and prototype observations.

Rock armour stability results from earlier model tests under non-depth-limited long-crested head-on waves are reviewed.

Results from new 2-D and 3-D model tests, carried out at Aalborg University, are presented. The tests were performed on detached low-crested breakwaters exposed to short-crested head-on and oblique waves, including depth-limited conditions. A formula that corresponds to initiation of hydraulic damage and allows determining armour stone size in shallow water conditions is given together with a rule of thumb for the required stone size in depth-limited design waves.

Rock toe stability is discussed on the basis of prototype experience, hard bottom 2-D tests in depth-limited waves and an existing hydraulic stability formula. Toe damage predicted by the formula is in agreement with experimental results. In field sites, damage at the toe induced by scour or by sinking is observed and the volume of the berm is often insufficient to avoid regressive erosion of the armour layer.

Stone sinking and settlement in selected sites, for which detailed information is available, are presented and discussed.

© 2005 Elsevier B.V. All rights reserved.

Keywords: Rock armour; Stability; Low-crest; Breakwater; Damage; Scour; Trunk; Roundhead; Toe

1. Introduction

Low-crested structures (LCSs) are defined as structures designed to be significantly overtopped by waves. LCSs are used in ports for protection of outer basins where wave transmission by overtopping is acceptable. However, most typically LCSs are used in shallow water as detached breakwaters for coastal protection purposes. The structures are usually built parallel to the shoreline and consequently exposed to wave attack almost perpendicular to the structure due to refraction of the waves. The shallow water conditions make the structure exposed to design waves numerous times during the structure lifetime. As damage is cumulative it is important to design for low or no damage. Design recommendations are therefore given corresponding to initiation of damage under design wave conditions.

For conventional breakwaters only a small amount of energy is allowed to pass over the structures. Damage will therefore mainly happen to the front slope. In case of LCSs the damage can occur also to the crest and the rear slope. However, because wave energy will pass over the structure, the LCSs are relatively more stable with the consequence that smaller armour stones can be used compared to the front armour of non-overtopped structures. The freeboard R_c , defined in Fig. 1, is therefore important for the stability.

In shallow water it is important to evaluate the breakwater stability for all relevant combinations of water levels and waves. In this respect, it should be noted that the impacts from non-breaking, breaking and broken waves are different.

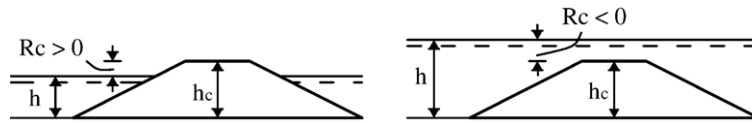
The aim of this paper is to describe the stability of detached LCS breakwaters based on new experimental results and field observations performed within the DELOS Project.

The paper is composed of seven main parts. Section 2 reviews former experimental results on hydraulic armour stability exposed to long crested non-depth-limited waves. Section 3 presents the results of new 3D-tests on armour stability in depth-limited short crested waves carried out at Aalborg University.

DOI of the original article: [10.1016/j.coastaleng.2005.09.001](https://doi.org/10.1016/j.coastaleng.2005.09.001).

* Corresponding author.

E-mail addresses: burcharth@civil.auc.dk (H.F. Burcharth),
alberto.lamberti@unibo.it (A. Lamberti).

Fig. 1. Definition of freeboard $R_c = h_c - h$.

Section 4 provides and discusses a new formulation for armour stability based on these 3D-tests. Section 5 examines hydraulic stability in case of depth-limited waves, provides a rule of thumb and compares it to some representative real design cases and to results of new 2D-tests performed at Aalborg University. Section 6 discusses structure design in depth-limited wave conditions. Section 7 deals briefly with the problem of toe hydraulic stability. Section 8 discusses the seabed effects on structure stability and presents some observations and surveys in selected sites, showing that structure-foundation interaction may be in several cases the cause of settlement and armour damages. Some design conclusions related to this problem are finally drawn.

2. Earlier trunk and roundhead armour stability tests in non-depth-limited waves

Van der Meer (1988) carried out 2-D model tests with LCSs exposed to non-breaking irregular waves. The cross-section is given in Fig. 2.

The water depth was kept constant 0.40 m. Three values of $R_c = -0.10, 0.00$ and $+0.125$ m were tested. The significant wave height H_s varied between 0.083 and 0.219 m. Two values of peak wave period T_p of approximately 2.0 and 2.6 s were applied. In each test series of approximately five tests, the T_p was kept constant while H_s was increased in steps, each one consisting of 3000 waves. Damage was characterized by the dimensionless damage parameter $S = A_e / D_{n50}^2$ by Broderick (1983), where A_e is the averaged cross-section eroded area and D_{n50} is the median equivalent cube length of the stones. As profiling of the armour surface were made also after 1000 waves the damage development could be studied. However, no simple and reliable prediction formula, as the one for non-overtopped slopes ($S \propto \sqrt{\text{number of waves}}$) was found for LCSs.

Givler and Sørensen (1986) performed stability tests of the structure shown in Fig. 3 under regular wave attacks.

Based on analysis of the Van der Meer (1988) and the Givler and Sørensen (1986) tests, Van der Meer and Pilarczyk (1990) proposed the following formula for the stability of LCS trunks exposed to head-on waves

$$\frac{h_c}{h} = (2.1 + 0.1S) \exp(-0.14N_s^*) \quad (1)$$

where $N_s^* = \frac{H_s}{AD_{n50}} s_p^{-1/3}$ is Ahrens (1984) spectral stability number, H_s is the significant wave height incident on the

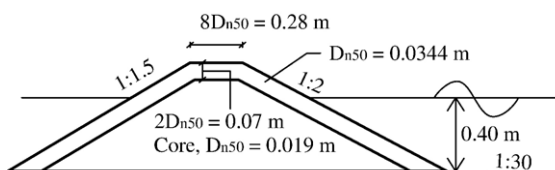


Fig. 2. Cross-section of Van der Meer (1988) tests.

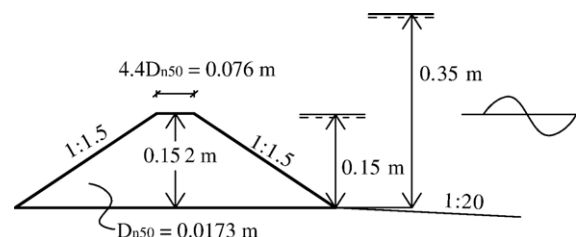
structure, $\Delta = (\rho_s / \rho_w) - 1$ is the buoyancy reduced relative density, ρ_s is the stone mass density, ρ_w is the water mass density, $s_p = H_s / L_p$ is the wave steepness at the structure toe and L_p is the wavelength at the structure toe associated to the peak period of incident waves.

The data set covers a wide range of test conditions, structure geometry, stone size and type of waves.

Vidal et al. performed model tests at National Research Council (NRC) Canada with a model including both trunk and roundheads. Trunk stability is reported in Vidal et al. (1992) and the roundhead stability in Vidal et al. (1995). The model is shown in Fig. 4.

Water depth varied between 0.38 and 0.65 m. The heights of the structure were 0.40 and 0.60 m and the range of the tested R_c between -0.05 and $+0.06$ m. Irregular long-crested waves perpendicular to the trunk with H_s between 0.05 and 0.19 m were used combined with two spectral peak periods, $T_p = 1.4$ and 1.8 s. The related number of waves in a test series was 3000 and 2600, respectively.

Vidal et al. (1992) divided the structure into several sections in order to study the distribution of the damage. It should be noted that the definition of crest in these tests contained the upper parts of the two slopes. A steel frame was covering the surface of the structure along the sections and a steel mesh was covering the parts where damage was not measured. Damage interactions among the sections were thereby not possible, e.g., damage to the crest section could not influence damage to the seaward slope section and vice versa. Further the steel frame restricted stones from movements along the boundaries within the sections. These effects most probably stabilized the stones making the sections in the experiments more stable than for real structures. As seen from Fig. 4, Vidal et al. (1992) also studied the response of a complete trunk section without steel mesh covering. The test results are presented in terms of diagrams showing various levels of damage for the studied parts of the structure as functions of the stability number $N_s = \frac{H_s}{AD_{n50}}$ and the dimensionless freeboard R_c / D_{n50} . Fig. 5 shows the diagram corresponding to initiation of damage. The figure points out that the trunk crest was the least stable part in case of submerged structures and that the leeward part of the head was the least stable part under emergent conditions.

Fig. 3. Cross-section of Givler and Sørensen (1986) tests. Range of R_c from 0 to -0.20 m.

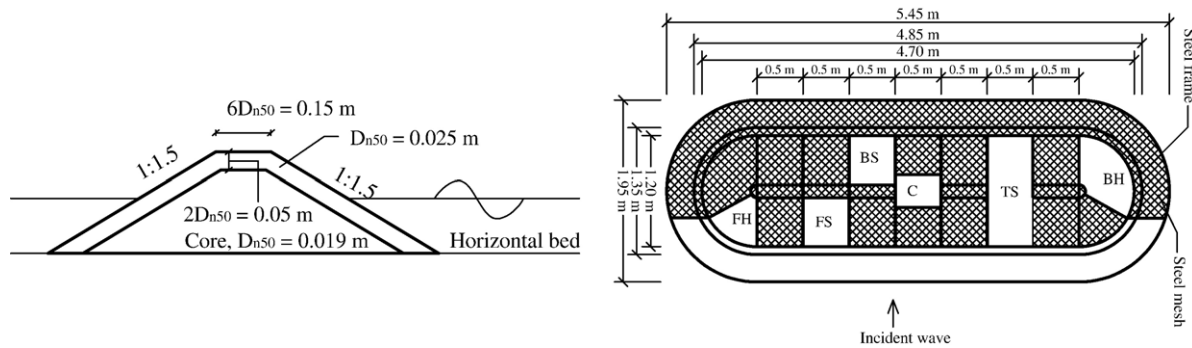


Fig. 4. Plan view and cross-section of model by Vidal et al. (1992).

Burger (1995) performed new flume experiments on trunk stability and re-analysed the existing tests reported by Van der Meer (1988) and Vidal et al. (1992). The analysis is described in detail in Burger (1995). The trunk was divided in seaward slope, crest and leeward slope. Stability, related to initiation of damage, was reported both for each sector and for the total trunk sector, see Fig. 6. From the figure it is evident that the crest is the least stable part of the trunk under submerged and slightly emergent conditions. For an emerged breakwater the seaward slope is the least stable part.

Burger (1995) investigated the influence of rock shape and grading on the stability of a slightly emerged LCS and concluded that the influence was very small especially for low damage levels: a rock type with relatively many elongated/flat rocks showed stability similar to more uniform rock types; no influence was found for gradings D_{85}/D_{15} smaller than about 2, and it was recommended not to use $D_{85}/D_{15} > 2.5$ ($M_{85}/M_{15} > 16$). The conclusion was to release customary strict limitations on shape or grading of armour material.

3. Armour stability tests in depth-limited short-crested waves

3.1. Test set-up and test conditions

Kramer and Burcharth (2003) performed within the DELOS project 3-D model tests at the Hydraulics and Coastal Engineering Laboratory, Aalborg University, Denmark. Both trunk and roundhead stability were studied. Fig. 7 shows a

photo of the model in the wave basin. A two meter wide 1:25 foreshore and a 0.5 m horizontal plateau were arranged in front of the trunk. The different coloured parts are used to distinguish where damage occurs.

Fig. 8 shows the two tested cross-sections with the different colouring of the parts of the structure. Both seaward and leeward slopes were 1:2. Crest widths of $3 D_{n50}$ and $8 D_{n50}$ were studied. A detailed description of the test set-up is given in Kramer et al. (2005) included in this Special Issue.

The ρ_s of quarry rock armour stones was 2.65 t/m^3 . Four values of $R_c = -0.10, -0.05, 0.0$ and 0.05 m were tested. Irregular 3D JONSWAP type waves with peak enhancement factor 3.3 were generated using the cosine power spreading function with spreading parameter $s = 50$, see Mitsuyasu et al. (1975). Two wave steepnesses of 0.02 and 0.035 and angle of incidence in the range -30° to $+20^\circ$ were generated (0° corresponding to the perpendicular to the trunk).

Time domain analyses showed that the wave heights followed closely the distributions predicted by the point model of Battjes and Groenendijk (2000), which takes into account foreshore slope and water depth at the structure. Fig. 9 shows an example of a wave height distribution H recorded in 0.25 m water depth at the toe of the structure for deepwater, with $H_s = 0.125 \text{ m}$ and $s_{op} = 0.02$ where s_{op} is the wave steepness associated with the incident H_s at the structure toe and the peak period deep water wavelength.

In each test series the wave height was gradually increased in steps each containing 1000 waves. Digital video and photos were used to identify displacements of armour stones.

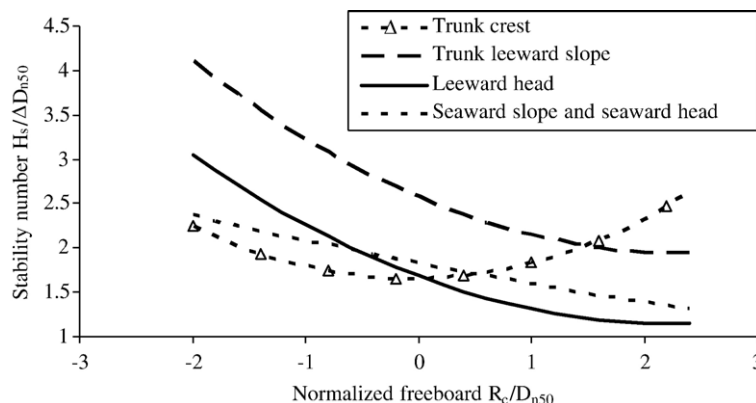


Fig. 5. LCS armour stability corresponding to initiation of damage Vidal et al. (1992, 1995). Non-depth-limited waves perpendicular to the trunk.

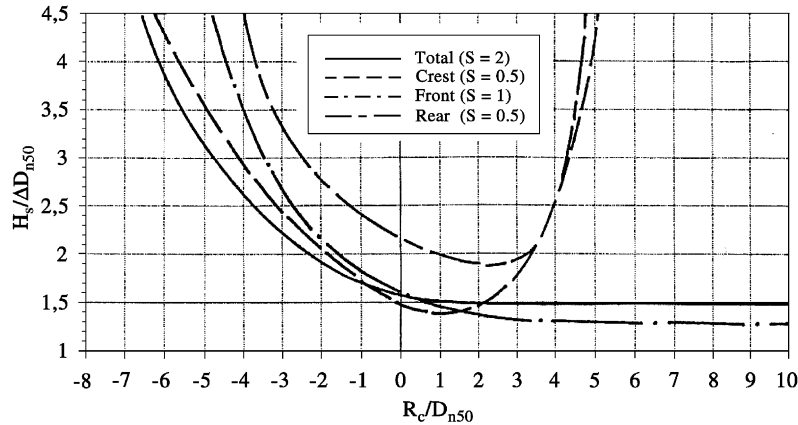


Fig. 6. Trunk armour stability corresponding to initiation of damage based on model test by Van der Meer (1988) and Vidal et al. (1992). Non-depth-limited waves, Burger (1995).

3.2. Observed damage

Initiation of damage corresponds to the state when a few stones start to be displaced. Table 1 indicates the observed location displacements in head-on waves for damage initiation (Kramer and Burcharth, 2003).

At the roundhead, the location of damage initiation shifted slightly with varying wave direction, see Fig. 10 for slightly emergent crest.

3.3. Definition of damage parameters

In order to compare the observed damage given as number of displaced armour stones N , to the Broderick parameter S for trunk damage, a link between N and S must be established. The eroded volume in the test section is $V_e = N \cdot D_{n50}^3 / (1 - n)$, where n is the porosity of the armour layer. Since $A_e = V_e / X$, where X is the width of the trunk section, we obtain

$$S = \frac{N \cdot D_{n50}}{(1 - n)X} \quad (2)$$

that, with the actual values of D_{n50} , $X = 0.50$ m and $n = 0.44$, gives $S = 0.11 \cdot N$.

To characterize the roundhead damage, the method by Vidal et al. (1995) is adopted. They observed, in agreement with the results presented here, cf. Table 1, that the region most prone to damage was between levels $(SWL + H_s/2)$ and $(SWL - H_s)$ and suggested that the reference width for damage quantification is calculated as the arch length $R \cdot \theta$, where R is the mean of the head radius corresponding to the two levels and θ is the angle of actual sector of the roundhead. In analogy with (2), the roundhead damage can then be expressed as

$$S_{\text{head}} = \frac{N \cdot D_{n50}}{(1 - n)R \cdot \theta} \quad (3)$$

where

$$R = \frac{B}{2} + \begin{cases} \frac{H_s + R_c}{2} \cdot \cot \alpha, & R_c \leq \frac{H_s}{2} \\ \left(\frac{H_{sc}}{4} + R_c \right) \cdot \cot \alpha, & R_c \geq \frac{H_s}{2} \end{cases} \quad (4)$$

α is the slope angle and B the crest width.

3.4. Definition of initiation of damage

For the trunk, initiation of damage was taken as $S = 0.5$ for each section, seaward slope, crest and leeward slope, differ-

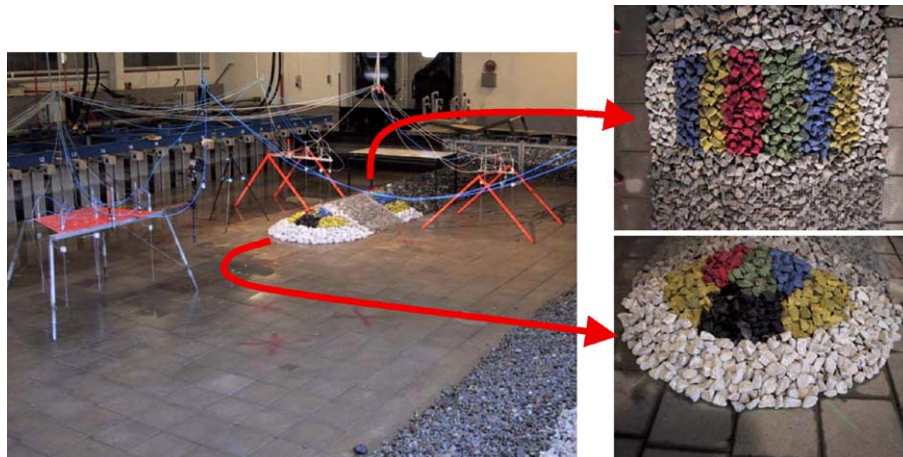


Fig. 7. Sections for observation of roundhead and trunk damage in the 3D-tests at Aalborg University, Denmark. For further information see also the companion paper by Kramer et al. (2005).

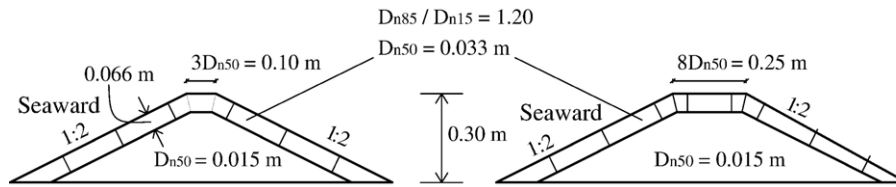


Fig. 8. Trunk cross-sections.

ently from what done by other researchers ($S=1$ for the seaward slope only in Fig. 6). This value of S corresponds to approximately four displaced stones in the 50 cm wide observed area.

For the roundhead, initiation of damage was chosen as $S=1$ for each of the three 60° sectors, cf. Table 1, since there was no reason for differentiation.

Narrow LCSs built in shallow water are only few stone-sizes high and wide at the crest. One stone removed from the edge of the crest causes a significant hole in the structure. For such small structures it is therefore chosen to define initiation of damage for the whole structure when just one section reaches this stage.

In these experiments S is calculated from the observed N of displaced stones, cf. (2) and (3). The evaluated damage therefore disregards settlements which otherwise increase the S -values.

3.5. Results and conclusions

Fig. 11 shows the results of the armour stability tests for the trunk and the roundhead with varying structure freeboard, incident wave direction and steepness.

The applied ranges of H_s/h corresponding to damage initiation are given in Table 2.

It is seen that the observed damage initiation corresponds for the tested structure to the range $H_s/h=0.25-0.4$ for the trunk and $H_s/h=0.25-0.60$ for the roundhead. This shows that in most cases the damage to the tested structure starts before H_s reaches the maximum depth-limited heights, which,

for the given foreshore slope and the applied wave steepnesses, would be approximately $H_s=0.6 \cdot h$. Only when the crest is relatively deeply submerged ($R_c/D_{n50}<4$) the waves could grow to their depth-limited maximum height without causing damage to the main armour. This is not a general rule but is a characteristic of the tested structure and of structures with D_{n50}/h lower than in the present tests. Structure response for larger values of D_{n50}/h is discussed in Section 5.

From Fig. 11 the following conclusions can be drawn.

Influence of wave direction. Head-on waves seem to produce more damage to the trunk than oblique waves. The difference in stability for positive and negative wave direction (see Fig. 10 for definition) is probably due to diffraction and model effect related to the position and the space for the 3-D wave recording array. For the roundhead, there seems to be little influence of wave direction on the threshold value of damage.

Influence of wave steepness. Both at trunk and roundhead the armour stability slightly decreases with increasing wave steepness.

Influence of crest width. No clear difference in stability between the two tested crest widths is observed.

4. Armour hydraulic stability formula

If the same size of rock armour is used for trunk slopes, crest and roundheads and design is based on the damage level corresponding to initiation, it is possible to derive from these experimental results a new armour stability formula.

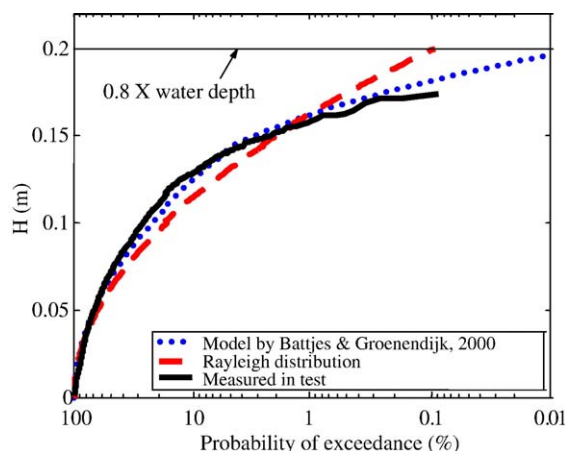


Fig. 9. Example of comparison of wave height distributions (Kramer and Burcharth, 2002).

Table 1

Location of initial armour displacements in head-on waves, marked with filled black areas

Freeboard	Damage to trunk	Damage to roundhead
$R_c > 0$ slightly emergent crest		
$R_c = 0$		
$R_c < 0$ submerged crest		

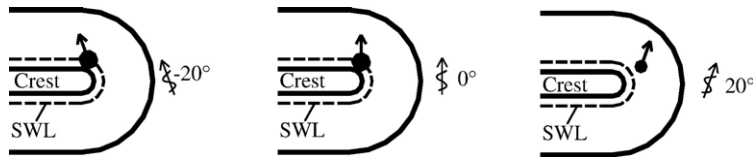


Fig. 10. Influence of wave angle of incidence on location of damage initiation at roundhead.

Fig. 12 shows all the trunk and roundhead data available from the tests at NRC Canada described by Vidal et al. (1992), at Delft Hydraulics described by Burger (1995) and at Aalborg University (labelled AAU 2002) described by Kramer and Burcharth (2003). The three sets of tests differ with respect to structure slope and waves (slope 1:1.5 and non-depth-limited 2-D waves in NRC 1992 and Delft 1995 tests; slope 1:2 and depth-limited short-crested waves in AAU 2002 tests). However, it happens that the effect of these differences compensates each other if only initiation of damage in some part of the structure is considered. This is indicated in Fig. 12, bottom right, by the lower envelope curve given by the

following stability formula (5), which represents the initiation of damage in some part of the structure

$$\frac{H_s}{\Delta D_{n50}} = 0.06 \left(\frac{R_c}{D_{n50}} \right)^2 - 0.23 \frac{R_c}{D_{n50}} + 1.36, \quad (5)$$

Eq. (5) assumes the same armour layer size for the whole structure and is valid for $-3 \leq R_c/D_{n50} < 2$ and slope 1:1.5 exposed to non-depth-limited waves, and slopes 1:2 exposed to depth-limited short-crested waves.

It can be expected that initiation of damage for slopes of 1:1.5 exposed to depth-limited short-crested waves corresponds to lower stability numbers than given by Eq. (5).

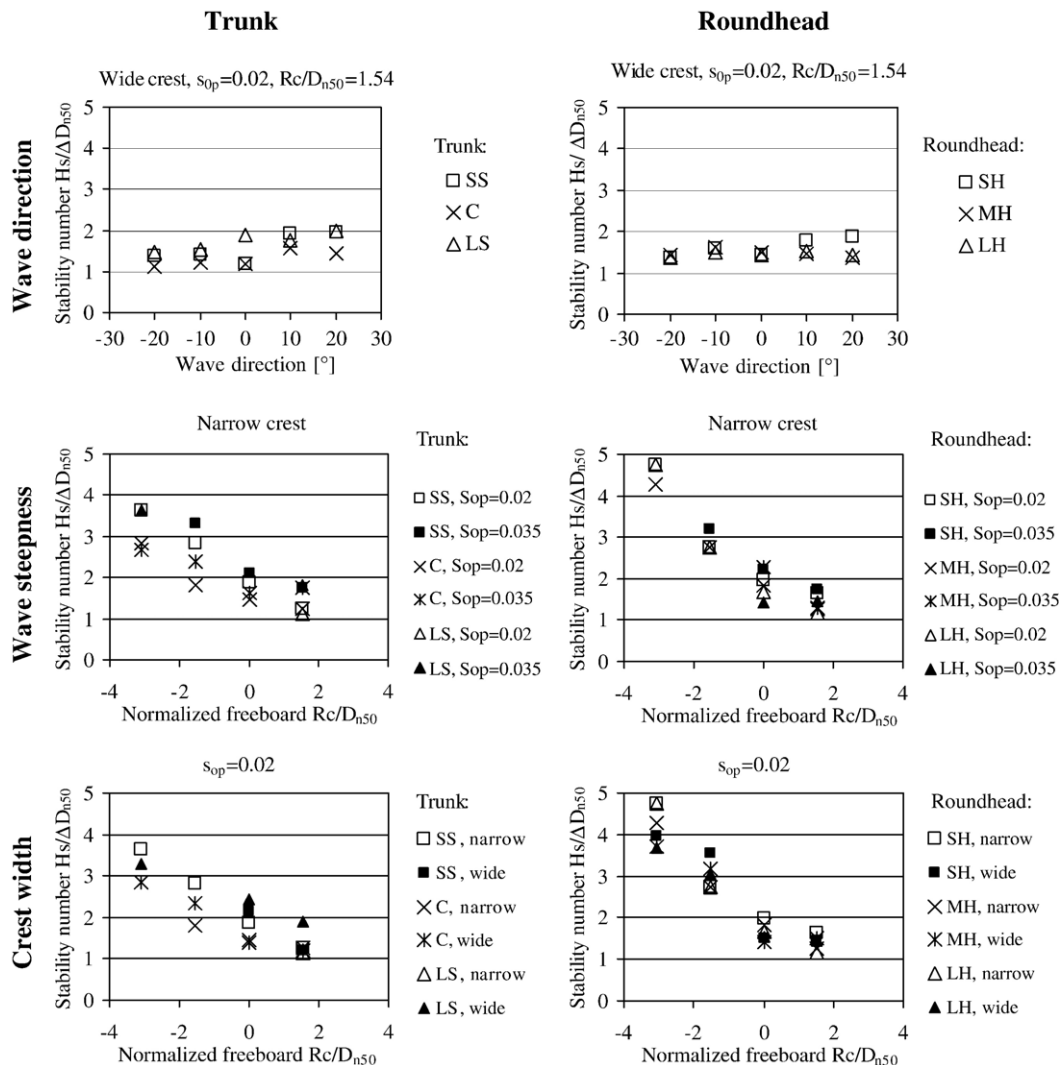


Fig. 11. Initiation of damage. Results of 3-D armour stability tests with low-crested breakwater in shallow water (Kramer and Burcharth, 2003). Legend: SS seaward slope, C crest, LS leeward slope, SH seaward roundhead (60° sector), MH middle roundhead (60°), LH leeward roundhead (60° sector).

Table 2

Ratios of H_s to water depth at the structure h corresponding to initiation of damage

Water depth h (m)	0.40	0.35	0.30	0.25
R_c/D_{n50}	−3.03	−1.51	0	+1.51
$\frac{H_s}{h}$ for trunk	0.35–0.40	0.30–0.35	0.25–0.30	0.25–0.35
$\frac{H_s}{h}$ for roundhead	0.50–0.60	0.40–0.50	0.25–0.30	0.25–0.35

For structures in deeper water, a differentiation in stone sizes for the various parts of the structure may be feasible. In such cases, the detailed model test results must be used for the design. The same holds if the design is based on damage levels more severe than initiation of damage.

5. Armour size in case of depth-limited waves

An equivalent equation for the most critical condition in depth-limited waves can be derived by considering the relationship between H_s and R_c :

$$H_s = \gamma h = \gamma(h_c - R_c) \quad (6)$$

where the factor γ depends on the seabed slope and the wave steepness.

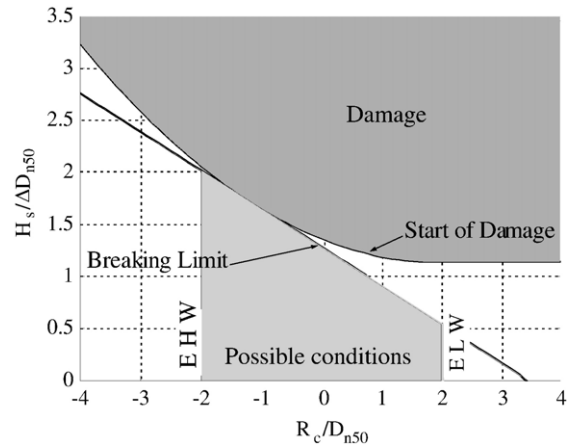


Fig. 13. Stability condition in depth-limited waves. Solid line is Eq. (5) extended beyond the minimum as a constant. Dashed line is Eq. (6) scaled with ΔD_{n50} and satisfying condition (7) for $\gamma=0.6$ and $\Delta=1.62$; its slope is γ/Δ and its intersection with the x -axis represents zero water depth conditions: $R_c=h_c$. EHW and ELW denote Extreme High and Low Water conditions, respectively; their value is site specific, the figure shows just a sample case.

Since the failure zone shown in Fig. 13 is the convex domain above Eq. (5), stability is assured for all water levels and for one level it is just at start of damage condition if (5) is

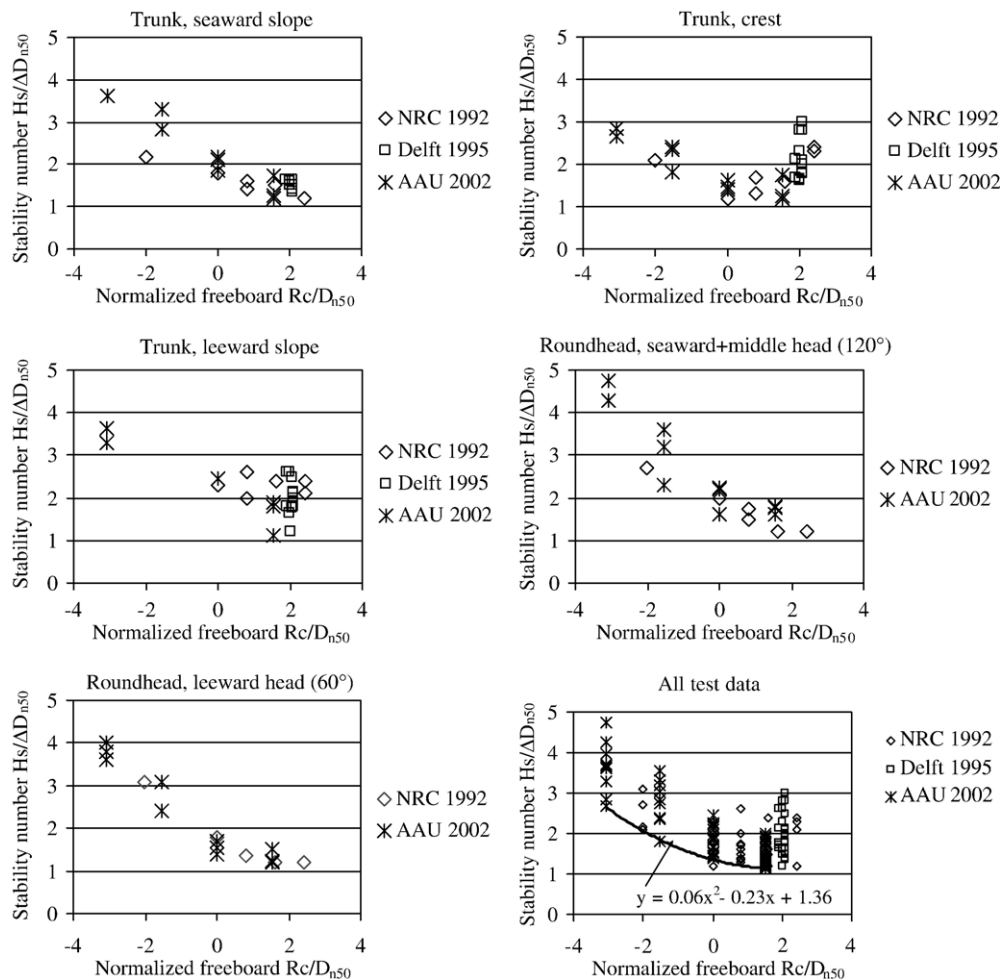


Fig. 12. Comparison of armour stability results (Kramer and Burcharth, 2002).

Table 3
Minimum stability for different degrees of submergence

Foreshore slope	$\gamma = \frac{H_s}{h}$	$\frac{R_c}{h_c}$	$\frac{D_{n50}}{h_c}$	$\frac{H_s}{\Delta D_{n50}}$
1/∞	0.40	−0.02	0.18	1.39
1/200	0.45	−0.08	0.21	1.46
1/100	0.50	−0.16	0.23	1.5
1/40	0.55	−0.25	0.26	1.6
1/20	0.60	−0.36	0.29	1.7
–	0.65	−0.48	0.33	1.8
–	0.70	−0.64	0.37	1.9

The γ -values are evaluated according to Van der Meer (1990) with $s_{op}=0.03$, $h/L_{op}=0.05$.

tangent to (6), i.e. if the discriminant of the combined (5) and (6) second order equation is zero, from which:

$$\frac{D_{n50}}{h_c} = \frac{\gamma/\Delta}{1.36 - (\gamma/\Delta - 0.23)^2/(4 \cdot 0.06)} \quad (7)$$

Results of Eq. (7) for different values of γ and $\Delta=1.6$ are reported in Table 3. The minimum stability for a given stone size occurs at slightly submerged conditions, i.e., negative R_c .

Design graphs can be extracted from Eq. (5) providing stone size for different h_c and R_c and given ρ_s , see an example in Fig. 14. The most critical conditions correspond in this case to $R_c = -0.36 \cdot h_c$, i.e., slightly submerged conditions.

For a gentle foreshore slope the following simple rule of thumb (RoT) is found

$$D_{n50} \geq 0.29 \cdot h_c \quad (8)$$

The flat maxima of the graphs in Fig. 14 indicate that the simple rule is valid for a fairly wide range of submergence.

Eq. (5) has been verified against the performance of a number of existing prototype structures (from the DELOS inventory described in Lamberti et al., 2005) as listed in Table 4. A good agreement between predictions by Eq. (5) and structure responses is observed.

Besides this validation, a series of new 2D model tests were performed at the Hydraulics and Coastal Engineering Laboratory at Aalborg University (Kramer, 2005) to verify the simple design rule. The cross-section of the tested structure, exposed to depth-limited waves, is shown in Fig. 15.

The ρ_s of the rock and toe armour was 2.65 t/m^3 . The total height of the structure was approximately, $h_c = 3.5 \cdot D_{n50} = 17 \text{ cm}$ corresponding to $D_{n50} = 0.29$ as given by (8). The water depth was increased in nine steps from 0.04 to 0.34 m. Waves with $T_p = 1.8 \text{ s}$ were used together with the maximum possible wave heights at the structure corresponding to the actual water depth. Wave reflection compensation was used together with two triple wave gauge arrays. The incident waves at the structure were depth-limited with H_s in the range 0.43 to 0.51 times h .

Damage to main armour and toe was recorded using digital photos taken before and after runs of approximately 1000 waves.

The tests showed that no displacements of main armour took place until water depth reached $h=0.23 \text{ m}$ corresponding to $R_c = -0.35 \cdot h_c$ and $R_c/D_{n50} = -1.2$, and in this case only one

stone in the upper part of the front armour was displaced corresponding to initiation of damage. An increase in the water depth did not result in more damage. This result confirms the simple rule (8) and shows that (5) can be used for depth-limited waves.

The toe was stable for all tested water depths.

6. Structure design in depth-limited wave conditions

The ratio D_{n50}/h_c imposes restrictions to the structure design.

A double armour layer with $D_{n50}/h_c > 0.5$ requires that part of the armour and the whole filter are placed below the natural bed level. This could be beneficial anyway if sea bed erosion is foreseen, see Fig. 16.

A value of $D_{n50}/h_c \cong 0.3$ implies that there is not sufficient space for a conventional core as the armour must rest directly on coarse filter material, see Figs. 16 and 17.

It should be noted that Eq. (5) is based on tests with sea side slope 1:2. For milder slopes smaller armour stones can presumably be stable and thus smaller values of D_{n50}/h_c are obtained; this is for instance the case of Ostia, where the structure slope is 1:5.

The derivation of the RoT (7) or (8) assumes that the critical submergence, $R_c/h_c \cong -0.36$, is within design conditions. The required stone size is however flat around the critical conditions and the RoT can be applied to a fairly wide range of submergence; it should not be applied to emergent breakwaters or coastal defence structures, that can deviate significantly from the RoT. The Elmer case in Table 4 is for instance one of these.

Only when $D_{n50}/h_c < 0.2$ there is space for a conventional core and filter layers. Moreover, the minimum filter thickness reduces as the armour size goes down.

7. Toe berm hydraulic stability

The function of a toe berm is to support the main armour layer and to prevent damage resulting from scour. Armour units

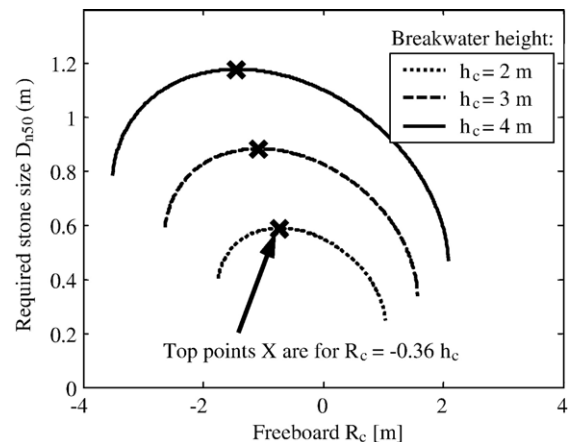


Fig. 14. Example of design graphs corresponding to damage initiation in case of depth-limited waves on gentle foreshore slope, $\gamma=0.6$ and $\rho_s=2.65 \text{ t/m}^3$.

Table 4
Validation of the Rule of Thumb (RoT), Eq. (8), and of Eq (5)

Breakwater	D_{n50} [m]	h_c [m]	R_c [m]	h [m]	D_{n50}/h_c	Satisfies	
						RoT, Eq. (8)	Eq. (5)
DK, Lønstrup	0.80	2.3	+1.3	1.0	0.34	✓	✓
DK, Skagen	0.71	2.0	+1.0	1.0	0.34	✓	✓
GR, Lakopetra	1.00	4.0	+0.7	3.3	0.25	÷ ^a	✓
GR, Alaminos	1.10	3.5	+0.5	3.0	0.32	✓	✓
GR, Paphos	1.40	4.5	−0.3	4.8	0.31	✓	✓
UK, Elmer	1.45	6.0	+4.3	1.7	0.24	÷ ^b	✓
UK, Monk's Bay	1.31	3.7	+2.2	1.5	0.36	✓	✓
ES, Altafulla	1.31	4.5	+0.5	4.0	0.29	✓	✓
ES, Comin	0.87	3.0	+0.5	2.5	0.29	✓	✓
ES, Postiguet	0.57	2.0	−2.0	4.0	0.29	✓	✓
ES, Palo	0.91	2.8	−1.5 to −2.0	4.3 to 4.8	0.32	✓	✓
IT, Punta Marina	0.90	2.8	−0.2	3.0	0.32	✓	✓
IT, Lido di Dante	0.80	2.5	−0.5	3.0	0.32	✓	✓
IT, Cesenatico	0.90	2 to 2.5	−0.5	2.5 to 3.0	0.36 to 0.45	✓	✓
IT, Ostia (1990)	0.50	2.5	−1.8 to −2.0	4.0	0.20	÷	÷ ^c
IT, Ostia (2003)	0.90	3.0	−1.0	4.0	0.30	✓	✓
IT, Sirolo	0.90	2.5 to 4.0	−1.0	3.5 to 5.0	0.23 to 0.36	÷	÷ ^d
IT, Scossicci	0.99	4.20	−1.0	5.20	0.24	÷	÷ ^d
IT, Grottammare	0.90	1.6	−0.9	2.5	0.56	✓	✓
IT, Bisceglie	1.04	2.55 to 4.15	−0.15	2.7 to 4.3	0.25 to 0.40	(÷) ^e	✓
IT, Nettuno	0.86	2.5	−0.5	3.5	0.34	✓	✓
IT, Amendolara	1.36	2.3	−0.5	2.8	0.59	✓	✓
IT, Pellestrina	0.76	2.5	−1.5	4.0	0.30	✓	✓

^a GR, Lakopetra: $H_{s, \text{design}} = 2.4$ m occurring during the design water depth $h \approx 4$ m corresponding to approximately $R_c = 0$ m. For this event $N_s = 1.4$, which satisfies Eq. (5).

^b UK, Elmer: Extreme high water depth $h = 5.4$ m corresponding to freeboard $R_c = +0.6$ m. The maximum significant wave height is estimated as $H_s = 0.6 \cdot h = 3.2$ m corresponding to $N_s = 1.4$. This is slightly more than the stability number calculated by Eq. (5). The Elmer structures have gentle slopes of 1:2.5 and wider roundheads, which makes the structures more stable than calculated by (5).

^c IT, Ostia: The 1990 breakwaters do not satisfy neither the RoT nor Eq. (5); structure slope is however 1/5 and stability of armour was checked in model tests.

^d IT, Sirolo and Scossicci: Damage to some structures experienced. Some structures have been rebuilt. The breakwaters do not satisfy neither RoT nor Eq. (5).

^e IT, Bisceglie. $H_{s, \text{design}} = 2.8$ m occurring when water depth $h = 5.1$ m corresponding to freeboard $R_c = -1.0$ m. For this event $N_s = 1.6$, which satisfies Eq. (5).

displaced from the armour layer may come to rest on the toe berm, thus increasing toe berm stability.

In shallow water and depth-limited design wave heights, support of the armour layer at the toe is ensured either by placing one or two extra rows of main armour units at the slope toe or by the use of stones or blocks in the toe that are smaller than the main armour, c.f. the examples of prototype structures given in Figs. 16 and 17. These solutions have shown to be stable. However, if more severe scour occurs very close to the structure and undermine the toe, the armour might slide. In such cases dedicated scour protection might be necessary, Sumer et al. (2005), or the toe berm must be wide enough to avoid this problem. The volume of the berm shall be such that its material is sufficient to protect the scour/erosion hole from further erosion without destabilising the armour layer slope,

i.e., its width should be around three times the erosion depth and its thickness at least four times its maximum stone size (rephrased after SPM, 1984). In this way slid berm stones can form, although dispersed, a stable and continuous slope covering the sand bed.

Toe berm stability is affected by wave height, water depth over the top of the toe berm, width of the toe berm and block size density; wave steepness does not appear to be a critical stability parameter.

Model tests with irregular waves indicate that the most unstable location is at the berm edge. The instability of a toe berm will trigger or accelerate the instability of the main armour. Aminti and Lamberti (1996) showed that moderate toe berm damage has almost no influence on armour layer stability, whereas high damage of the toe berm severely reduces the

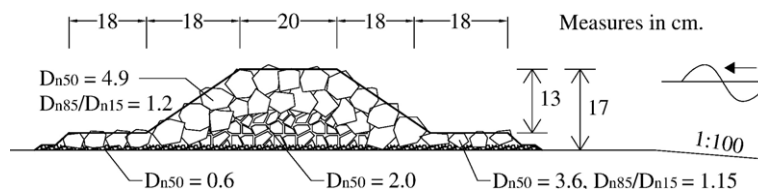


Fig. 15. Cross-section of breakwater tested in irregular depth-limited waves at Aalborg University. $D_{n50}/h_c = 0.29$.

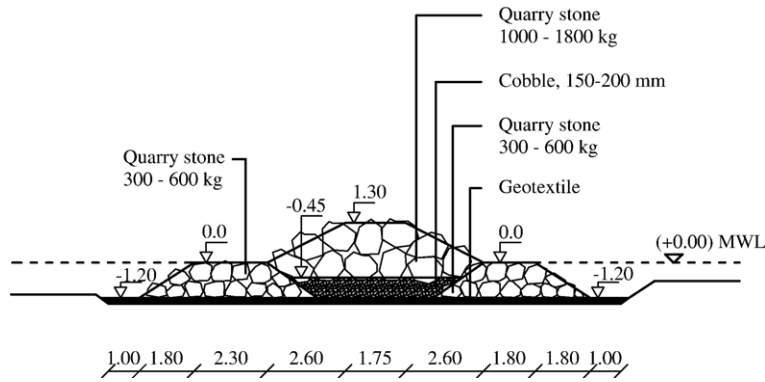


Fig. 16. Cross-section of breakwaters at Lønstrup, Denmark (Lastrup and Madsen, 1994). $D_{n50}/h_c \cong 0.34$.

armour layer stability. In practice it is economical to design toe berms that allow for little or no damage.

No model tests dealing especially with toe berm stability of LCSs exist. However, within DELOS a few model tests on LCSs with depth-limited waves and wave breaking at the toe showed good agreement with the formula for trunk toe stability of emerging breakwaters given in the following subsection by Eq. (9). For LCSs wave energy can pass over the structure making them more stable than the conventional type. Seaward toe berms designed by formulae developed for non-overtopped breakwaters will therefore be more conservative when used for LCSs, as it is confirmed by the model tests performed within DELOS. These tests showed that the seaward toe is more prone to hydraulic damage than the leeward one, indicating that it is safe to apply the same stone type in the leeward toe as calculated for the seaward toe. Further, these tests proved that oblique incident wave attacks produce less damage than orthogonal ones.

7.1. Toe berm stone sizes in trunk

The following formula (9) by Van der Meer et al. (1995) predicts the required rock size for the toe berm at the trunk

$$N_s = \frac{H_s}{\Delta D_{n50}} = \left(0.24 \frac{h_b}{D_{n50}} + 1.6 \right) N_{od}^{0.15} \quad (9)$$

where h_b is the water depth at the top of toe berm and N_{od} is the number of units displaced out of the armour layer within a strip

of width D_{n50} . For a standard toe size about 3–5 stones wide and 2–3 stones high:

$$N_{od} = \begin{cases} 0.5 & \text{no damage} \\ 2 & \text{acceptable damage} \\ 4 & \text{severe damage} \end{cases}$$

For a wider toe berm, higher N_{od} values can be applied.

The formula (9) was developed for sloping, emergent rubble mound breakwaters. Stones having a $\rho_s = 2.68 \text{ t/m}^3$ were used and the berm width was varied.

The formula is valid for non-breaking, breaking and broken head-on irregular waves; its validity field can be identified by the ranges: $0.4 < h_b/h < 0.9$, $0.28 < H_s/h < 0.8$, $3 < h_b/D_{n50} < 25$.

During the tests on the model shown in Fig. 15 exposed to maximum depth-limited waves in water depths 4–34 cm, no displacements of the toe stones took place. The parameter intervals for the tests are within the ranges of validity of (9), but also values of h_b/D_{n50} down to zero were tested. By using the test conditions, Eq. (9) gives $N_{od} = 0–0.10$ which corresponds to almost no displacement and is thus in agreement with test results.

7.2. Toe berm stone sizes at roundheads

For the toe berm at the roundhead no specific recommendations exist. In many situations, previous experiences can be used to evaluate the necessary size of the rocks. Rock sizes equal to the ones of the trunk might be used, but in that case it is recommended to validate the design by the use of model tests.

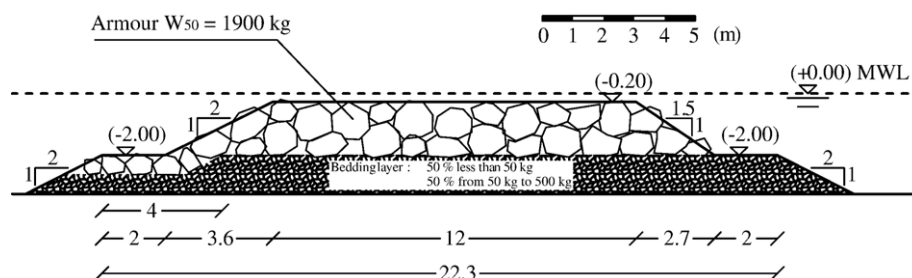


Fig. 17. Cross-section of submerged breakwaters at Punta Marina, Emilia Romagna coast, Italy. $D_{n50}/h_c \cong 0.32$.

When the LCS length to gap ratio is great and its freeboard is close to zero, intense rip currents at the gaps do occur. This might affect the toe stability especially if scour takes place in front of the toe. If model tests are used to design the toe berm it is very important that in the experiments rip currents and mobility of the bed are correctly modelled/scaled.

If the toe is located in very shallow water and it is expected to be very exposed, then the same stone type as used in the main armour layer of the roundhead can be applied. This will always lead to a conservative design where units are not displaced by waves and currents.

8. Prototype experience

8.1. Discussion of seabed effects

It is worth noting that the above design formulae are empirically derived from fixed-bed models. In real field conditions the seabed foundation is typically highly mobile, consisting in most cases of fine sands subjected to intense hydrodynamic action.

Indeed the observed prototype damage of the rubble mound (as described by Lamberti et al., 2005) is often the consequence of geotechnical or morphodynamic instabilities rather than hydraulic response. First of all, the simple dumping of stones onto the sand bed causes sinking and settlements, especially when proper bottom protection is not used. Moreover, breaking waves and the related strong nearshore currents tend to produce local scour (see Sumer et al., 2005) and deposition near the structure toe, which affect the toe stability either directly (e.g., scour sliding) or indirectly (variation in local water depth and thus changes of incident wave height). Finally, sand intrusion and infilling plus ecological colonization can strongly reduce the structure porosity and wave energy absorption properties.

Generally to avoid sinking of the rubble stone material into a sandy seabed it is necessary to separate the two materials by the use of small stone filter layers, geotextiles or mattresses.

Consolidation and settlement of the seabed material and the stone rubble cause lowering of the crest. If these processes terminate during construction the rubble mound volume must be oversized; if they last longer than the construction then the structure must be designed and initially built higher. The necessary increase in crest elevation (in the following termed *overheight*) depends on the seabed characteristics, the height of the structure and the construction method. For example a high rubble mound structure built on a muddy seabed by means of floating equipment demands a large overheight to compensate for a long-term settlement. On the other hand a low rubble mound structure placed on a coarse sandy seabed by land-based equipment running on already placed materials, demands much less overheight as settlement will be small and almost completed during construction.

In the following subsections, damages to structures in some Italian DELOS case studies are presented (for the description of sites and works, refer to Lamberti et al., 2005). Both Ostia and Pellestrina design were checked by means of physical model

tests in primary hydraulic laboratories, see Ferrante et al. (1992) or the quoted report Delft Hydraulics (1989), and Consorzio Venezia Nuova (1990).

8.2. Observations in Ostia, Italy

The submerged LCS structure built in 1990 on a sandy seabed with $D_{50}=0.20$ mm and foreshore slope 1:250 (cross-section in Fig. 6, Lamberti et al., 2005) has been reshaped in time by settlements, with an average crest lowering of 0.5 m in one decade. A computation of the actual “damage” was made by comparing negative differences (eroded areas) of barrier cross-sections with the “as built” geometry resulting from the 1992 survey. The average damage over the six representative sections is plotted in Fig. 18. There is an evident tendency to equilibrium with a maximum mean damage of 12.5% in nine years starting with a damaging rate around 2.5% per year and ending around 0.6% per year. A progressive barrier siltation from both shoreward and offshore transport has reduced the rock barrier porosity and its energy dissipation efficiency, and increased its reflectivity.

The 1990 design was tested in a 2D mobile bed hydraulic model at a scale 1:15 and “showed a remarkable stability of the rock barrier”, Ferrante et al. (1992).

In conclusion the LCS, after settlement (despite geotextile), had a weak protection effect due to its low crest elevation (average of -2.3 m MSL), requiring maintenance of the 1990 works performed in steps in 2001 and 2003–4 by the placement of 1–3 t rock, in order to raise the crest up to design levels of -1.0 and -0.5 m MSL and by beach nourishments.

Franco et al. (2005) question about the hydraulic stability of the barrier and apparently relate the observed damage to hydraulic reshaping of the breakwater estimated according to Van der Meer (1990) formulae. Eq. (1) explains actually only a small fraction of the observed crest lowering (0.1 m). It should be concluded that the prevailing mechanism of crest lowering is barrier settlement due to bed mobilisation (not properly represented in the model tests).

8.3. Observations in Pellestrina, Italy

Despite this important intervention was verified by means of a physical model test and resulted globally effective, a barrier

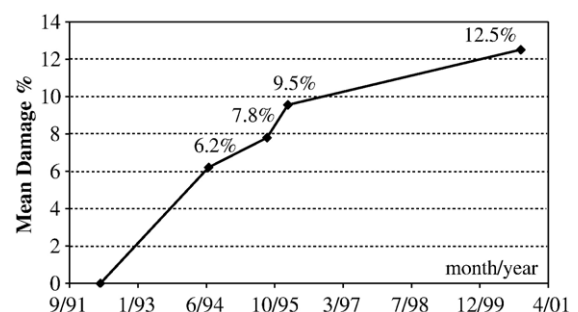


Fig. 18. Ostia submerged breakwater mean damage. From Franco et al. (2005).

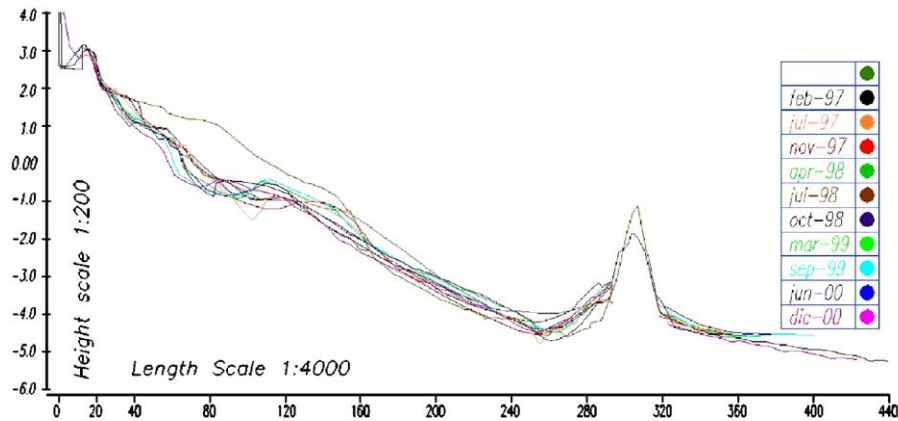


Fig. 19. Cross-shore profiles in cell 1 of the Pellestrina barrier surveyed by Consorzio Venezia Nuova. The green line corresponds to the survey just after the works. The blue line corresponds to the 2000 survey.

settlement of about -0.4 m in around five years occurred, as it can be derived from the cross-shore profiles shown in Fig. 19 for cell 1, the most southern cell of the barrier, constructed in 1995 (the map of the complete scheme and the barrier cross-section are shown in Fig. 9 in Lamberti et al., 2005). The characteristic D_{n50} of the sandy bottom is 0.20 mm and foreshore slope is around $1:100$. The sandy bottom rests around depth -15 m a.s.l. over a thick layer of over-consolidated clays.

From the multi-beam survey of cell 9 (the central one of the barrier) performed in October 2002 (see Fig. 3 in Zyserman et al., 2005) the same average barrier settlement of -0.4 m in five years is found. From the other multi-beam survey performed in October 2002 at the southernmost oblique breakwater, close to cell 1, it can be derived an average settlement of -0.2 m.

Local scour at the inshore roundhead side of the southern breakwater, discussed in depth in Sumer et al. (2005), is recognizable in Fig. 20 together with the possible sliding of some stones of the inshore slope.

In conclusion the barrier suffered only very limited and local damages but a settlement around -0.4 m in 5 years is

observed. Even though no maintenance works have been performed, the barrier continues to function properly.

8.4. Observations in Lido di Dante, Italy

The barrier, initially completed in 1997 (cross-section shown in Fig. 10 in Lamberti et al., 2005), was re-charged in June 2001 using 2380 m³ of natural rock, in order to compensate for the lowering of the structure due to settlement into the bed and to some armour rock displacements caused by wave impacts. Another rock recharge, which brought the crest level just slightly emerging from mean sea level, was performed in June 2004. The average structure settlement can be estimated to about -0.5 m in four years. The sandy seabed is characterized by a $D_{n50}=0.18$ mm. The foreshore slope is around $1:160$.

Deep crescent-shaped erosion at the inshore roundhead side causing some stone displacements appears evident in the bathymetric rendering shown in Fig. 21.

During the DELOS ecological monitoring of the barrier, the ecologist group observed that some stones (around $1:10$)

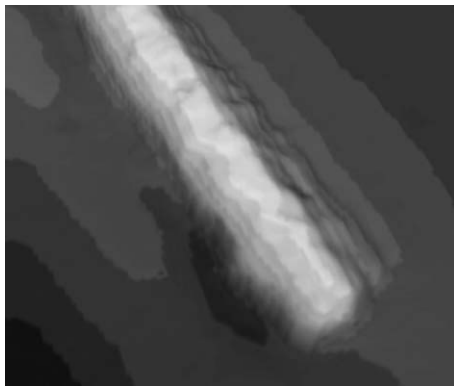


Fig. 20. 3D-view of the Pellestrina barrier southern roundhead. Multi-beam survey of October 2002 performed by the University of Bologna. Waves come from the right boundary. The dark area just inside the head indicate a region of scour.

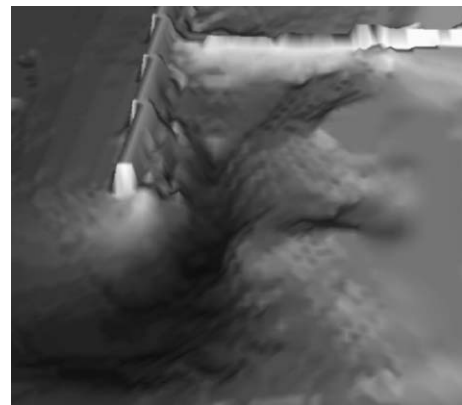


Fig. 21. Crescent-shaped erosion at the roundhead of the northern barrier at Lido di Dante, Italy. Multi-beam survey performed by the University of Bologna in June 2002. Waves come from the left boundary, the beach is to the right. A groin connects the barrier with the shore.

marked for collecting samples in the intertidal region were moved or rolled down.

According to Table 4 and accounting for the milder foreshore slope, the armour of the Lido di Dante barrier should be hydraulically more stable than the Pellestrina one. This however is contradictory to the observations: the Lido di Dante structure experienced more sinking. This can be due to insufficient filter functionality with consequent settling of the toe and dilation of the armour slope. Due to the narrower crest, the toe settling may induce a more evident settlement of the entire structure.

9. Conclusions

A new design formula corresponding to the state of damage initiation for rock armoured low-crested structures exposed to depth-limited waves is presented. The formula is valid for armour slope 1:2 and is based on 3-D model tests in short-crested waves.

Considering the differences in models and test conditions, the formula fits the test data by Vidal et al. (1992) and Burger (1995) for initiation of damage for low-crested structures with armour slope 1:1.5 exposed to long-crested waves.

Within the tested ranges, effects of crest width, wave steepness and obliquity are small; whereas the influence of the freeboard is large: submerged LCSs are much more stable than emerged ones under the same waves.

In case of depth limited waves slightly submerged conditions are the most critical with respect to armour stability. Corresponding to such conditions a simple rule of thumb is presented according to which the nominal diameter for rock with mass density 2.65 t/m^3 should be approximately 20% to 30% of the height of the structure, dependent on foreshore slope and wave steepness. This rule has been tested against new 2-D model tests and performance of several prototype structures examined in DELOS through the LCS inventory.

The validity of the toe-berm stability formula by Van der Meer et al. (1995) has been verified by comparison to a few model tests in depth limited waves, and a good agreement was found.

Prototype existing structures suggest that the armour hydraulic stability is not the only and most critical failure mode of LCSs. A proper (wide and stable) toe protection, blocking regressive erosion at the bed, and a proper, well-placed filter avoiding structure settlement in the sandy bed are equally important conditions for long term stability. Since LCS efficiency is very sensitive to submergence, settlement may bring the structure out of the acceptable functioning domain.

Field observations in Ostia, Pellestrina and Lido di Dante document a barrier settlement variable in the range 3 to 15 cm/year, with the greatest values occurring immediately after the works on fine sandy bottoms. In these cases there is no evident correlation between the hydraulic stability of the armour layer and the structure settlement.

Settlement process is only imperfectly understood, appears to be underestimated in mobile bed physical model tests and deserves more attention in future research and design applications.

Notations

γ	Breaker index (H_s/h) in depth-limited wave conditions, depending on seabed slope and offshore wave steepness
Δ	$=(\rho_s/\rho_w) - 1$ Relative density
ρ_s	Stone mass density
ρ_w	Water mass density
A_e	Averaged cross-section eroded area
D_{n50}	Median equivalent cube length of the stones
H_s	Significant wave height
h	Water depth at the structure toe
h_b	Water depth at the top of toe berm
h_c	Structure height
L_{op}, L_p	Wavelength associated to peak wave period off-shore or at the structure toe
N	Number of displaced armour stones
N_{od}	Number of units displaced out of the armour layer within a strip width of D_{n50}
N_s^*	Ahrens (1984) spectral stability number
n	Porosity of the armour layer
R_c	Structure freeboard
S	Broderick parameter S for trunk damage
s	Spreading parameter
s_{op}, s_p	Wave steepness off-shore, at the structure toe
T_p	Peak period
V_e	Eroded volume in the test section
X	Width of the trunk section

Acknowledgements

The authors acknowledge the comments by Prof. L. Franco, University of Rome 3, Dr. J.W. van der Meer, Infram ltd, and Prof. C. Vidal, Universidad de Cantabria.

This study has been partially funded by the Commission of the European Commission, Research-Directorate-General, Contract Nr. EVK3-2000-00041, "Environmental Design of Low Crested Coastal Defence Structures" (DELOS).

References

- Ahrens, J.P., 1984. Reef type breakwaters. Proc. 19th Coastal Engineering Conference, Houston, U.S.A.
- Aminti, P., Lamberti, A., 1996. Interaction between main armour and toe berm. ASCE Proc. ICCE 1996, vol. 2, pp. 1542–1555.
- Battjes, J.A., Groenendijk, H.W., 2000. Wave height distributions on shallow foreshores. Coastal Engineering 40, 161–182.
- Broderick, L.L., 1983. Riprap stability, a progress report. Proc. Coastal Structures '83. American Society of Civil Engineering, pp. 320–330.
- Burger, G., 1995. Stability of low-crested breakwaters. Final Proceedings, EU research project Rubble mound breakwater failure modes, MAST 2 contract MAS2-CT92-0042. Also published in Delft Hydraulics report H1878/H2415.
- Consorzio Venezia Nuova, 1990. Technical Report on the Preliminary Project of Venice Littoral Defence Works from River Brenta to Sile Part of the New Interventions for Venice Safeguard (in Italian). Report VE0706 PMRT 01, vol. 1. TECHNITAL, Verona.
- Delft Hydraulics, 1989. Coastal protection plan, Lido di Ostia: morphologic study. Report H891.
- Ferrante, A., Franco, L., Boer, S., 1992. Modelling and monitoring of a perched beach at Lido Di Ostia (Rome). Proc. ICCE 1992, vol. 3, pp. 3305–3318.

- Franco, L., Di Risio, M., Riccardi, C., Scaloni, P., Conti, M., 2005. Monitoraggio del rinascimento protetto con barriera sommersa nella spiaggia di Ostia Centro. *Studi Costieri* 8, 3–16.
- Givler, L.D., Sørensen, R.M., 1986. An investigation of the stability of submerged homogeneous rubble mound structures under wave attack. H.R. IMBT Hydraulics Report IHL-110-86. Lehigh University.
- Kramer, M., 2005. Structural Stability of low-crested breakwaters. PhD thesis. Hydraulics and Coastal Engineering Laboratory, Aalborg University, ISSN 0909-4296, SERIES PAPER NO. 26, in press.
- Kramer, M., Burcharth, H.F., 2002. Wave basin experiment final form, 3-D stability tests at AAU. Report of DELOS EVK-CT-2000-0004/.
- Kramer, M., Burcharth, H.F., 2003. Stability of low-crested breakwaters in shallow water short crested waves. *Proc. Coastal Structures '03*, Portland, Oregon, U.S.A., pp. 139–149.
- Kramer, M., Zanuttigh, B., Van der Meer, J.W., Vidal, C., Gironella, F.X., 2005. Laboratory experiments on low-crested breakwaters. *Coastal Engineering* 52 (10–11), 867–885.
- Lamberti, A., Archetti, R., Kramer, M., Paphitis, D., Mosso, C., Di Risio, M., 2005. Prototype experience regarding low-crested structures. *Coastal Eng.* 52 (10–11), 841–866.
- Lastrup, C., Madsen, H.T., 1994. Design of breakwaters and beach nourishment. 24th Internal Conference on Coastal Engineering, 1994. ASCE, Kobe, Japan, pp. 1359–1372.
- Mitsuyasu, H., Tasai, F., Suhara, T., Mizuno, S., Ohkusu, M., Honda, T., Rikishi, K., 1975. Observations of directional spectrum of ocean waves using a cloverleaf buoy. *Journal of Physical Oceanography* 1, 750–760.
- SPM, 1984. Shore Protection Manual, 4th edition. US Army Corps of Engrs, Coastal Engng. Res. Center, US Govt Printing Office, Washington DC.
- Sumer, M., Fredsøe, J., Lamberti, A., Zanuttigh, B., Diken, M., Gislason, K., Di Penta, A., 2005. Local scour and erosion around low-crested structures. *Coastal Engineering* 52 (10–12), 995–1025.
- Van der Meer, J.W., 1988. Rock slopes and gravel beaches under wave attack. *Delft Hydraulics Communication*, vol. 396.
- Van der Meer, J.W., 1990. Extreme shallow water wave conditions. Report H198. Delft Hydraulics Laboratory, The Netherlands.
- Van der Meer, J.W., Pilarczyk, K.W., 1990. Stability of low-crested and reef breakwaters. *Proc. 22nd International Conference on Coastal Engineering*, Delft, The Netherlands, pp. 1375–1388.
- Van der Meer, J.W., Angremond, K.d., Gerding, E., 1995. Toe structure stability of rubble mound breakwaters. *Proceedings of the Advances in Coastal Structures and Breakwaters Conference*. Institution of Civil Engineers, Thomas Telford Publishing, London, UK, pp. 308–321.
- Vidal, C., Losada, M.A., Medina, R., Mansard, E.P.D., Gomes-Pina, G., 1992. An universal analysis for the stability of both low-crested and submerged breakwaters. *Proc. 23rd International Conference on Coastal Engineering*, Italy, pp. 1679–1697.
- Vidal, C., Losada, M.A., Mansard, E.P.D., 1995. Stability of low-crested rubble mound breakwater heads. *Journal of Waterway, Port, Coastal, and Ocean Engineering* vol. 121, No. 2. ASCE, pp. 114–122.
- Zyserman, J., Johnson, H.K., Zanuttigh, B., Martinelli, L., 2005. Far field erosion and morphological effects. *Coastal Engineering* 52 (10–11), 977–994.